

Chain Conformation of Poly(alkylene oxide)s Studied by Small-Angle Neutron Scattering

Christine Gerstl,[†] Gerald J. Schneider,^{*,‡} Wim Pyckhout-Hintzen,[†] Jürgen Allgaier,[†] Sabine Willbold,[§] Diana Hofmann,^{§,||} Ulrich Disko,^{⊥,||} Henrich Frielinghaus,[‡] and Dieter Richter[†]

[†]Jülich Centre for Neutron Science JCNS and Institute for Complex Systems ICS, Forschungszentrum Jülich GmbH, 52425 Jülich, Germany

[‡]Jülich Centre for Neutron Science JCNS-FRM II, Outstation at FRM II, Forschungszentrum Jülich GmbH, 85747 Garching, Germany

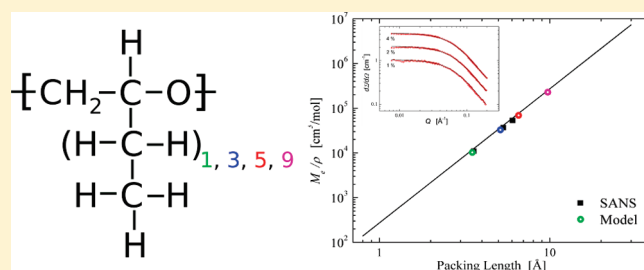
[§]Zentralabteilung für chemische Analyse, Forschungszentrum Jülich GmbH, 52425 Jülich, Germany

[⊥]Institut für Bio- und Geowissenschaften, Forschungszentrum Jülich GmbH, 52425 Jülich, Germany

^{||}BIOSPEC, Forschungszentrum Jülich GmbH, 52425 Jülich, Germany

S Supporting Information

ABSTRACT: Using small-angle neutron scattering, the unperturbed chain dimensions of a series of poly(alkylene oxide)s (PAO's) were studied as a function of side-chain length. The PAO's were obtained using anionic ring-opening polymerization methods. The deuterated monomers were synthesized from commercially available precomponents. A systematic decrease of the chain dimensions with increasing length of the side chains was found. We also compare the PAO's with the chemically very similar poly(olefin)s with respect to the characteristic ratio C_∞ , the chain dimensions, and the packing length as a function of the molecular weight per backbone bond. In doing so, we found significant differences between the static properties of the two systems.



INTRODUCTION

Studying the unperturbed chain dimensions has long been and still is a major topic in polymer science,^{1–8} and especially the homologous series of the poly(olefin)s has been studied extensively over the last decades.^{9–14} The poly(olefin)s have side chains of varying length and exhibit a systematic decrease of the glass transition temperature T_g with increasing length of the side chains.^{13–15} This is a feature reported also for other side-chain polymers, e. g. the poly(*n*-alkyl acrylate)s and poly(*n*-alkyl methacrylate)s.^{16–19} In contrast, the homologous series of the poly(alkylene oxide)s (PAO's) shows a virtually constant glass transition temperature.²⁰ Therefore, a detailed study of the chain conformation of the PAO's would be highly interesting. Up to now, the radius of gyration R_g of poly(butylene oxide) has been determined only in Θ -solvent a long time ago,² and in a recent study of poly(octylene oxide)–poly(ethylene oxide) diblock copolymers R_g of poly(octylene oxide) is given.²¹

Here we present the first ever systematic study of the unperturbed chain dimensions of a series of poly(alkylene oxide)s (PAO's). We used small-angle neutron scattering (SANS) to study the chain conformation of the PAO melts by using a mixture of protonated and deuterated polymers, focusing thereby on the variation of the length of the side chains. Below, we report the synthesis and characterization of deuterated monomers for three different PAO's. The resulting virtually monodisperse

samples together with previously synthesized protonated polymers²² now allowed for the first experimental exploration of the relation of the PAO-chain dimensions to molecular weight per backbone bond m_b : Various techniques were exploited to accurately determine the radius of gyration, and quantities like the packing length p and the characteristic ratio C_∞ are derived. The results are discussed in terms of the backbone equivalence model¹² and compared to the poly(olefin)s.

The paper is organized as follows. In the experimental section the polymer synthesis and sample composition is introduced, and the SANS method is presented. In the Theory section, a brief overview over the necessary scattering functions for the data modeling is given. Then in the Results and Discussion, the experimental results are presented and discussed.

EXPERIMENT

Polymer Synthesis and Analysis. *Materials.* 1-Bromobutane-*d*₉, 1-bromohexane-*d*₁₃, and 1-bromooctane-*d*₁₇ (all Isotec, 98 atom-% D), *N,N*-dicyclohexylmethylamine (Aldrich, 97%), 3-chloroperbenzoic

Received: June 7, 2011

Revised: July 12, 2011

Published: July 18, 2011

Table 1. Sample Details of the PAOs

sample	M_w [g/mol]	M_w/M_n	N_{mono}^a	ρ [g/cm ³] ^b
h-PBO	43 500	1.02	604	$0.98-7.2 \times 10^{-4}T$
d-PBO	39 800	1.04	497	$1.09-7.2 \times 10^{-4}T$
h-PHO	41 700	1.08	417	$0.94-6.9 \times 10^{-4}T$
d-PHO	36 800	1.03	329	$1.05-6.9 \times 10^{-4}T$
h-POO	9870	1.03	77	$0.92-6.6 \times 10^{-4}T$
d-POO	11 900	1.02	83	$1.04-6.6 \times 10^{-4}T$

^a Average number of monomers per polymer chain. ^b T in °C.

acid (Aldrich, 70.5% peracid), diethylene glycol dibutyl ether (Aldrich, $\geq 99\%$), and diethyl ether (Aldrich, $\geq 99\%$) were used as received.

General Synthetic Procedures. The deuterated monomers were synthesized from commercially available fully deuterated 1-bromoalkanes. In the first reaction step the 1-bromoalkanes were converted into the corresponding 1-alkenes by elimination of HBr. The deuterated 1-alkene oxide monomers were obtained by oxidizing the 1-alkenes using 3-chloroperbenzoic acid. The progress of the oxidation reaction was controlled by determining the residual peroxide via titration of samples taken at different times with the potassium iodide - sodium thiosulfate system. For the synthesis of the hydrogenous polymers commercially available 1-alkene oxide monomers were used. Before polymerization the monomers were dried over CaH₂ according to ref 22. The anionic ring-opening polymerizations of the alkene oxides were carried out using the potassium *tert*-butanolate (KOt-Bu) and 18-crown-6 (18C6) initiating system. The mass ratio of monomer to the solvent toluene ranged between 0.8 and 1.1 and a polymerization temperature between -10 and -15 °C. In the case of the two polyoctylene oxides (cf. Table 1), the molar ratio of 18-C-6 to KOt-Bu ranged between 0.8 and 0.9 and the polymerization time was between 4 and 6 days. For the other polymers the molar ratio of 18-C-6 to KOt-Bu ranged between 3.0 and 3.2 and the polymerization time was between 5 and 9 days. The details of the polymerization reactions are described in ref 22.

Monomer and Polymer Characterization. Gas chromatography–mass spectrometry: The low boiling alkene oxides were analyzed by GC-MS on an Agilent 6890-GC, coupled with a Finnigan MAT 95sq-MS. The samples were GC-separated on a SGE BPX5 column (25 m \times 0.22 mm \times 0.25 μ m) with adequate temperature programmes. The helium flow was 1 mL/min (electronic pressure control). The mass spectrometer was used in the electron ionization mode (70 eV, ion source temperature 260 °C). The observed mass range was 50–800 Da and the scan duration was 0.74 s. All fractions from the low temperature distillations were investigated by GC-MS in several dilution steps. All samples were injected considerably overloaded with respect to the main product in order to reveal traces of impurities originating, e.g., from side reactions or solvent impurities in full scan spectra. This is especially essential for highly reactive compounds, which interfere in the course of next reaction steps. A semiquantitative estimation was achieved in a more diluted case. Because of the lack of deuterated standards, neither external nor internal calibration was possible. The differences of the response factors under electron ionization mode are indeed negligible in contrast to the ESI ionization; but for the detection/integration of impurity peaks especially in the sub-%-range the main product has to be saturated and therefore a general overestimation of all minor products took place.

The NMR spectra were obtained on a Varian Inova 400 MHz. All samples were measured at 295 K in CDCl₃ with a 5 mmPFG AutoX DB Probe. Chemical shifts are given in δ ppm using the residual proton signal of the deuterated solvent as reference ($\delta_{\text{H}/\text{D}}(\text{CDCl}_3) = 7.24$ ppm; $\delta_{\text{C}}(\text{CDCl}_3) = 77$ ppm).

The SEC experiments were carried out using a PL-GPC 50 instrument. Three Polypore (Polymer Laboratories) 5 μ m columns (molecular weight operating range 200–2 000 000 g/mol) at 30 °C were used. For the signal detection a Viscotek Model TDA 300 detector with differential refractometer (RI) detector at 650 nm and a 90° laser light scattering (LS) detector at 670 nm was used at 30 °C. The solvent was THF at a flow rate of 1 mL/min, which was degassed with a Viscotek Model VE 7510 instrument. Molecular weights were calculated from the results of the LS and RI detectors using the Polymer Laboratories Cirrus GPC software. Molecular weight distributions were obtained using conventional polystyrene calibration.

1-Butene-*d*₈. First, 150.4 g of 1-bromobutane-*d*₉ (1.03 mol) was heated together with 301.2 g of *N,N*-dicyclohexylmethylamine (1.54 mol) for 27 h in a 1 L steel autoclave to 160 °C. Because of the formation of 1-butene the pressure increased to 14 bar. After the heating was finished the autoclave was connected to a vacuum line and the butene was cryodistilled under vacuum conditions into a pressure tested flask equipped with a Teflon stopcock. The crude product obtained was purified by another cryodistillation step. For this distillation the 1-butene was cooled to dry ice temperature and distilled at the vacuum line into another flask, which was kept at liquid nitrogen temperature. Thus, 28.1 g of 1-butene-*d*₈ (44%) was obtained. The purity of the product was not examined. Instead, it was assumed that it was similar to the product, which was obtained under identical reaction conditions using hydrogenous 1-bromobutane. In that case the product contained according to ¹H NMR 96% of 1-butene, 3% of 2-butenes, and 1% of hydrogenous cyclohexene.

1-Butene Oxide-*d*₈. First 118.1 g of 3-chloroperbenzoic acid containing 0.48 mol of peracid was dissolved in 280 g of diethylene glycol dibutyl ether. The mixture was cooled to dry ice temperature and was degassed at a vacuum line. Then 28.1 g of 1-butene-*d*₈ (0.44 mol) was distilled into the reaction flask. The mixture was first warmed up to 0 °C and within 3 days it was brought to room temperature, where it was left for another 4 days. The crude product was isolated by cryodistillation at a vacuum line, whereby the flask containing the reaction mixture was kept at room temperature and the crude product was collected in a flask cooled to liquid nitrogen temperature. After drying over Na₂SO₄ the crude product was purified by distillation using a 30 cm vacuum-jacketed column, packed with 3 \times 3 mm wire mesh rings (Normag). Prior to the distillation 5.7 g of toluene were added as a polymerization inert substance to the crude product in order to increase the yield in the distillation step. The fraction distilling between 62 and 62.5 °C was collected for the polymerization experiments.

The analysis by ¹H NMR showed the presence of <1% of toluene. In order to quantify the toluene content tetrabromoethane ($\delta = 6$ ppm) was added as a reference. The known weights of sample and reference allowed quantifying all present proton compounds. In the ²H NMR spectrum only the signals of 1-butene oxide could be detected. The GC-MS analysis revealed besides the main product 1-butenoxid-*d*₈ some toluene. Moreover, a very small peak at 14.7 min (0.2%) showed the presence of some 2-butenoxid-*d*₈.

1-Hexene-*d*₁₂. First, 200.4 g of 1-bromohexane-*d*₁₃ (1.12 mol) was heated together with 326.5 g of *N,N*-dicyclohexylamine (1.67 mol) for 7 h to 170–175 °C in a flask equipped with a reflux condenser. After the heating was finished the flask containing the reaction mixture was connected to a vacuum line and the hexene was cryodistilled under vacuum conditions into another flask. The crude product was purified by distillation using a 30 cm vacuum-jacketed column, packed with 3 \times 3 mm wire mesh rings (Normag). The fraction distilling between 61.5 and 65.5 °C was collected for the oxidation. Thus, 41.7 g of 1-hexene-*d*₁₂ (43%) was obtained.

Analysis by ¹H NMR showed the presence of 1% of hydrogenous cyclohexene. In the ²H NMR spectrum only the signals of 1-hexene could be detected. Signals of 2- and 3-hexenes were not visible. These results were confirmed by the ¹³C NMR spectra.

1-Hexene Oxide- d_{12} . First, 115.9 g of 3-chloroperbenzoic acid containing 0.47 mol of peracid was dissolved in 490 g of diethyl ether. The mixture was cooled to dry ice temperature, and 41.4 g of 1-hexene- d_{12} (0.43 mol) were added. The mixture was warmed up to 0 °C and was brought to room temperature overnight, where it was left for another 8 days. After that time the product mixture was washed with 10% aqueous NaHCO_3 in order to remove the residues of 3-chlorobenzoic acid and 3-chloroperbenzoic acid. It was neutralized by washing with saturated aqueous NaCl and dried over Na_2SO_4 . After removal of the diethyl ether the crude product was purified by distillation using a 30 cm vacuum-jacketed column, packed with 3×3 mm wire mesh rings (Normag). Prior to the distillation 16.2 g of *o*-xylene was added as a polymerization inert substance to the crude product in order to increase the yield in the distillation step. The fraction distilling between 117 and 119 °C was collected for further purification and the polymerization experiments. The analysis by ^1H NMR showed the presence of *o*-xylene, cyclohexene oxide, ethanol, ethyl acetate, and ethyl formate. The quantitative analysis of the ^1H NMR spectrum showed that all these compounds were found in amounts smaller than 0.5%. After the drying step over CaH_2 the product was analyzed by GC-MS. This investigation confirmed the existence of some *o*-xylene and cyclohexene oxide. The other impurities found in the NMR analysis, ethanol, ethyl acetate, and ethyl formate, were eliminated. However, additionally some chlorobenzene was detected. This compound was not found in the NMR analysis because of the small concentration and the partial overlap of the chlorobenzene signals with the chloroform signal. A more detailed description of the impurities detected by GC-MS is given in form of a table in the Supporting Information including substance identification, retention time, scheduler mass spectrum, and relative fraction beside the spectrum of the main component with interpretation.

1-Octene- d_{16} . First, 202.3 g of 1-bromooctane- d_{17} (0.96 mol) was heated together with 251 g of *N,N*-dicyclohexylamine (1.28 mol) for 13 h to 170–175 °C in a flask equipped with a reflux condenser. The further procedure was the same as described for the synthesis of 1-hexene oxide- d_{12} except that prior to the final distillation 12.1 g of *o*-xylene was added to the crude product. The fraction distilling between 117.5 and 124 °C was collected for the oxidation. Thus, 47.4 g of 1-octene- d_{16} (39%) were obtained. The analysis by ^1H NMR showed the presence of 1% of hydrogenous cyclohexene and 3% of *o*-xylene. In the ^2H NMR spectrum only the signals of 1-octene could be detected. Signals of 2-, 3-, and 4-octenes were not visible.

1-Octene Oxide- d_{16} . The procedures for the oxidation reaction were the same as described for the 1-hexene oxide- d_{12} synthesis using 97.0 g of 3-chloroperbenzoic acid (0.39 mol of peracid), 47.0 g of 1-octene- d_{16} (0.37 mol), and 390 g of diethyl ether. The overall reaction time was 11 days. After having added 5.5 g of decane the distillation was carried out at 300 mbar, and the fraction distilling between 122 and 124.5 °C was collected for further purification and the polymerization experiments. The analysis by ^1H NMR showed the presence of 13% decane and 3% *o*-xylene. After the drying step over CaH_2 the product was analyzed by GC-MS. Besides the deuterated octene oxide and the impurities already found in the ^1H NMR examination before, about 0.5% of deuterated heptene oxide was additionally detected.

Samples. Three different poly(alkylene oxide)s (PAO's) were studied, having side chains of two, four, and six carbon atoms per side chain. Their characteristics are summarized in Table 1. In each case, three different mixtures of deuterated material in a protonated matrix were measured, the percentages being approximately 1, 2, and 4%.

The mixtures were prepared in pentane solution, stirred thoroughly, and while still stirring dried under high vacuum. Under argon atmosphere, they were filled into Hellma sample cells with a thickness of 0.5 mm, which were then sealed with Teflon tape. A complete list of the measured sample compositions is given in Table 2.

Table 2. Sample Nomenclature^a

sample	ϕ [vol %]	sample	ϕ [vol %]	sample	ϕ [vol %]
PBO-1	0.89	PHO-1	0.91	POO-1	0.87
PBO-2	1.85	PHO-2	1.85	POO-2	1.76
PBO-4	3.69	PHO-4	3.54	POO-4	3.53

^a ϕ are the percentages of deuterated polymer in protonated matrix.

Instrument and Data Treatment. The SANS experiments were performed on the KWS-1 instrument of the Jülich Centre for Neutron Science (JCNS) at the FRM II research reactor in Garching, Germany.²³ The polymer mixtures were measured at three temperatures within a small range (i.e., $T = 280, 300,$ and 320 K). (Measurements at lower temperatures would not have been comparable because of the crystallization of POO, and because of the uncertain sealing of the sample cells higher temperatures could have led to a possible degradation of the polymers, rendering the whole experiment useless.) Three different setups with sample-to-detector distances of $L = 1, 2,$ and 8 m, a collimation length of 8 m, and wavelength $\lambda = 7$ Å were used. The wavelength spread was $\Delta\lambda/\lambda = 10\%$. With these setups, the scattering vector Q ranges from 7×10^{-3} to 0.25 Å⁻¹. The beam aperture was 10×10 mm². The raw data were corrected for scattering from the empty cell, detector sensitivity, and background noise. For measuring the latter, boron carbide is used to block the beam. Calibration in absolute units (cm⁻¹) is done by using a PMMA secondary standard:

$$\left(\frac{d\Sigma}{d\Omega}\right)_s = \frac{(L_s)^2 h_{pl} T_{pl} (d\Sigma/d\Omega)_{pl}}{(L_{pl})^2 h_s T_s T_{ec} \langle I_{pl} \rangle} ((I_s - I_{bc}) - T_s (I_{ec} - I_{bc}))$$

Here pl, s, ec, and bc refer to the PMMA standard, sample, empty cell, and boron carbide, respectively. T_x denotes the respective transmission, $I(Q)$ the scattered intensity, h the sample thickness, and L the sample-to-detector distance. $\langle I_{pl} \rangle = \langle (I_{pl} - I_{bc}) - T_{pl}(I_{ec} - I_{bc}) \rangle$ is the averaged measured intensity of the PMMA, with the intensity of the empty beam I_{ec} . All transmissions are measured with a monitor inside the beam-stop at $Q = 0$.

After radial averaging the incoherent contributions of both protonated and deuterated chains were subtracted in order to obtain the absolute coherent macroscopic differential cross sections $(d\Sigma/d\Omega)_{\text{coh}}(Q)$, hereafter abbreviated as $I_{\text{pol}}(Q)$. The correction for the incoherent background was realized by subtracting a constant $C_{\text{inc},0}$, assuming a power law description for the data at high Q . The subtracted constants agreed well with the calculated incoherent scattering of the samples.

THEORY

The scattering function of an ideal Gaussian chain in the discrete representation in the limit of infinite dilution is given by (e.g., in ref 24)

$$\begin{aligned} I_{\text{pol}}(Q) &= V \phi_{\text{pol}} (\Delta\rho)^2 S_{\text{pol}}(Q) \\ &= V \phi_{\text{pol}} (\Delta\rho)^2 \frac{1}{N_{\text{mono}}^2} \left\{ N_{\text{mono}} \frac{1+b}{1-b} - 2b \frac{1-b^{N_{\text{mono}}}}{(1-b)^2} \right\} \end{aligned} \quad (1)$$

where V is the volume of a polymer chain, ϕ_{pol} the polymer volume fraction, $\Delta\rho = \rho_1 - \rho_2$ the scattering contrast with ρ_i ($i = 1, 2$) the corresponding scattering length densities (=SLD) of polymer and matrix or Θ -solvent. $S_{\text{pol}}(Q)$ is the single chain structure factor, N_{mono} is the number of monomers and $b = \exp(-l^2 Q^2/6)$ with the statistical segment length l . $Q = (4\pi/\lambda) \sin(\vartheta/2)$ denotes the momentum transfer, where ϑ is the scattering angle.

For large N_{mono} (i.e., $\approx > 100$), $S_{\text{pol}}(Q)$ can be simplified to the Debye formula

$$S_{\text{Debye}}(Q) = \frac{2}{x^2} (x - 1 + \exp(-x)) \quad (2)$$

with $x = Q^2 R_g^2$, where the radius of gyration is given by

$$R_g^2 = \frac{\int r^2 \rho(\vec{r}) d^3r}{\int \rho(\vec{r}) d^3r} = \frac{1}{6} C_{\infty} n \langle l_0^2 \rangle \quad (3)$$

with distance from the center of mass r , SLD ρ , characteristic ratio C_{∞} , and backbone bond number $n = N_{\text{mono}} \cdot n_b$. There N_{mono} is the number of monomers per chain and n_b the number of backbone bonds per monomer. $\langle l_0^2 \rangle$ is the mean square of the different bond lengths l_0 in the backbone of one monomer ($(\langle l_0^2 \rangle)^{1/2} \approx 1.54 \text{ \AA}$ for C – C single bonds, and $\approx 1.43 \text{ \AA}$ for C – O single bonds²⁵).

Often, in a polymer isotope blend the protonated (“h”) and deuterated (“d”) species do not have the same degrees of polymerization: $N_h \neq N_d$. A standard approach to account for this and for the isotope interaction is by a random phase approximation:²⁴

$$\frac{\Delta\rho^2}{I_{\text{pol}}(Q)} = \frac{1}{\phi_h V_0 N_h S_h(Q)} + \frac{1}{\phi_d V_0 N_d S_d(Q)} - 2\chi/V_0 \quad (4)$$

where ϕ_i and N_i are the corresponding volume fraction and degree of polymerization of the two isotopes, V_0 is the average monomer volume, and χ the Flory–Huggins interaction parameter.

An independent way for obtaining R_g and χ is by a so-called Zimm analysis, i.e., plotting

$$\frac{\phi(1-\phi)}{N_A} \text{ vs } Q^2 - k\phi(1-\phi) \quad (5)$$

$$\frac{(\Delta\rho)^2 I_{\text{pol}}(Q)}{(\Delta\rho)^2 I_{\text{pol}}(Q)}$$

for small Q (i.e., $QR_g \leq 1$) and several concentrations ϕ yields χ (mol/cm^3) = $-(m_Q)/(2k)$ with a constant k and m_Q being the slope of the extrapolation $Q \rightarrow 0$, and $M_w = (N_A)/((\Delta\rho)^2 y_0)$ with the extrapolation’s y -axis intercept y_0 . Extrapolating $\phi \rightarrow 0$ gives the radius of gyration $R_g = (3V_{\text{chain}} m_{\phi})^{1/2}$ with the extrapolation’s slope m_{ϕ} .

RESULTS AND DISCUSSION

Hydrogenous polyalkylene oxides having narrow molecular weight distributions up to high molecular weights can be synthesized by anionic ring-opening polymerization.²² In contrast to the hydrogenous monomers, the deuterated analogues are not commercially available. They were synthesized using commercially available perdeuterated 1-bromoalkanes as starting materials. By eliminating HBr the corresponding 1-alkenes were obtained. It is compulsory to carry out this reaction with the help of a bulky base such as tertiary amines in order to suppress the subsequent isomerization by migration of the double bond. Besides the isomerization products of the 1-alkenes cyclohexene was found in the product mixtures. This compound is a decomposition product of *N,N*-dicyclohexylmethylamine, the amine base used for the dehydrobromination reaction. Therefore, careful distillation of the raw products was necessary to minimize the cyclohexene content. In the second reaction step the 1-alkenes were oxidized using 3-chloroperbenzoic acid. After

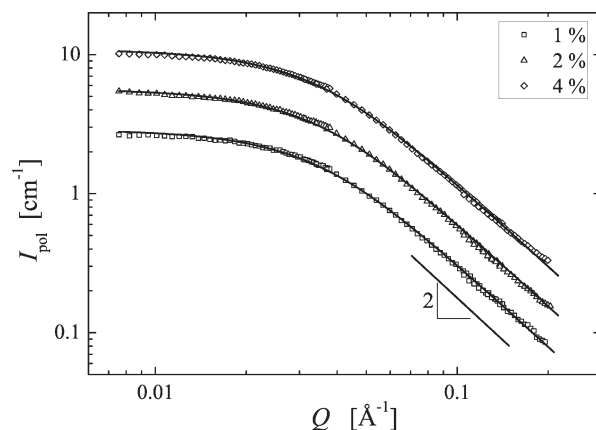


Figure 1. Simultaneous Debye fits (cf. eq 2) (lines) to the PHO samples (symbols) at 300 K. The error-bars of the data points are within the symbol size and are therefore left out for sake of clarity. The extra line represents the slope at high Q expected from the Debye approximation.

distillative purification of the 1-alkene oxides no more than traces of other isomers were found. Cyclohexene oxide was present only in 1-hexene oxide- d_{12} at a level of about 0.25%. Other impurities found in 1-hexene oxide- d_{12} were ethanol, ethyl acetate, and ethyl formate, which most likely originated from the solvent diethyl ether and were accumulated in the distillation process. In addition, in 1-hexene oxide- d_{12} small quantities of chlorobenzene were found. This compound originates from the peracid used in the oxidation steps. Except the chlorobenzene the other impurities could be fully eliminated in the drying process of the monomers over CaH_2 . However, the small quantities of chlorobenzene of not more than 0.05% had no influence on the polymerization processes. The molecular weight distributions of the deuterated polymers were comparable to the ones of the hydrogenous polymers and the measured molecular weights coincided within the experimental error with the expected values calculated from the amounts of monomer and initiator used (cf. Table 1).

It is a standard procedure to fit the SANS data with the Debye approximation, i.e., eq 2 multiplied with the forward scattering I_0 . Since PBO and PHO have relatively large degrees of polymerization, the Debye function can be used in these cases. As an example, Figure 1 shows the scattering curves of the three PHO mixtures on the absolute scale, measured at 300 K together with the Debye fits. The fits agree very well with the data points, which is true for both PBO and PHO, and all temperatures. This procedure yields the radius of gyration R_g of the minority component, which means in the present case that of the deuterated polymers. The R_g 's showed no significant and systematic change with temperature and were thus taken to be independent of temperature within the small range we studied (280 to 320 K). Therefore, the values, which can be found in Table 3, are averaged over the three temperatures.

For the rather short POO, which has only roughly 80 monomers, the discrete scattering function of a Gaussian chain eq 1 has to be used. Exemplary curves are shown in Figure 2. Also here, the R_g of the deuterated component is obtained. Additionally fitting PBO and PHO with eq 1 produced the same R_g values as eq 2, thereby showing that the use of the Debye approximation is well justified in these cases.

The slopes at high Q -values are proportional to Q^x with $x = -2.0 \pm 0.1$ for PBO, -1.9 ± 0.1 for PHO, and -1.7 ± 0.1 for

Table 3. Temperature Averaged R_g 's of the Deuterated Components from the Debye and Zimm Plots, eq 1, and RPA, and χ from the Zimm Plots and RPA

	PBO	PHO	POO
	Debye		
R_g [Å]	50.5 ± 0.1	42.8 ± 0.5	—
	eq 1		
R_g [Å]	50.5 ± 0.1	43.1 ± 0.5	23.26 ± 0.05
	Zimm		
R_g [Å]	53.7 ± 0.5	43.01 ± 0.05	23.2 ± 0.1
χ [mol/cm ³]	(− 2.25 ± 0.25) × 10 ^{−5}	(− 1.0 ± 0.5) × 10 ^{−5}	(4.6 ± 3.3) × 10 ^{−5}
	RPA		
R_g [Å]	48.0 ± 0.5	40.2 ± 0.5	19.5 ± 0.5
χ [mol/cm ³]	(4 ± 1) × 10 ^{−5}	(5 ± 1) × 10 ^{−5}	(29 ± 4) × 10 ^{−5}

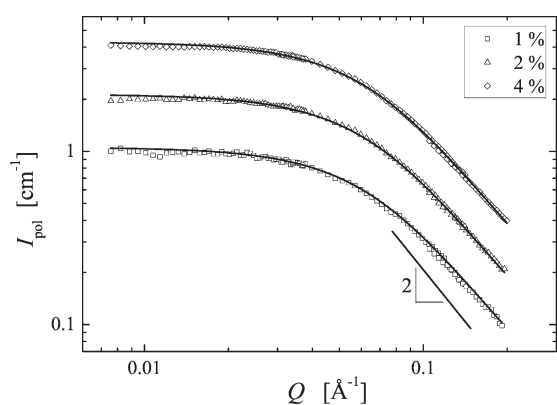


Figure 2. Simultaneous fits of eq 1 (lines) to the POO samples (symbols) at 320 K. The error-bars of the data points are within the symbol size and are therefore left out for sake of clarity. The extra line represents the slope at high Q expected from the Debye approximation.

POO. For PBO and PHO, this corresponds to the Debye prediction, and also for short chains the obtained value is reasonable, because the slope expected from the full scattering function is smaller than $Q^{-2.26}$.

In Figure 3, an exemplary Zimm plot (PBO@320 K) is shown. For all samples, the Q -range was chosen such that $QR_g \leq 1$. Being the low- Q expansion of the Debye function, the Zimm analysis is independent of the chain statistics at high Q and should therefore give reliable results for all PAO's. The obtained radii of gyration and Flory–Huggins interaction parameters χ are listed in Table 3. The R_g are again those of the deuterated component. The small values for χ indicate that the isotope interaction between protonated and deuterated polymer is insignificant.

Additionally, RPA fits according to eq 4 were performed. The radius of gyration of the deuterated component $R_{g,d}$ was coupled to the protonated polymers' $R_{g,h}$ via the known ratio of monomer numbers N_i ($i = h, d$), so that $R_{g,d} = R_{g,h}(N_d/N_h)^{1/2}$. The different concentrations were fitted simultaneously, and again no significant and systematic change with temperature was observed. Hence also in this case R_g and χ given in Table 3 are averaged over the three temperatures. The radii of gyration obtained from the RPA are uniformly a bit smaller than those from the other

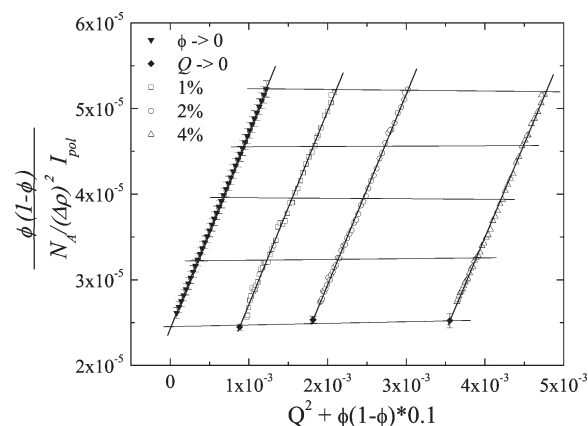


Figure 3. Zimm plot for PBO at 320 K. The error bars of the measured data points are within the symbol size and are therefore left out for sake of clarity. The quasi-horizontal lines express the negligible χ -parameter in the Zimm evaluation.

methods, while the χ values are somewhat larger. The latter, however, are again close to zero and it can thus be concluded that the above statement concerning the interspecies interaction holds. Because of the good quality of the fits, it is not possible to discern RPA and Debye fits by visual inspection, and therefore no additional picture is shown.

To judge the influence of the asymmetry in molecular weight of the protonated and deuterated components, a second RPA fit was done: the ratio of monomers was set to 1, and χ was fixed to the value obtained before. The resulting R_g did not differ within the error-bars from the one where the correct ratio was used. Therefore, we conclude that the difference in the degree of polymerization is small enough that it has no effect on the fitting parameters.

The R_g of POO has been measured before by Hamley et al.²¹ There, $R_g = 22.0 \pm 0.5$ Å independent of temperature (between 300 and 450 K) was obtained using $M_w(h) = 10100$ g/mol and $M_w(d) = 12150$ g/mol (this corresponds to an h-equivalent $M_{w,equiv} = 10800$ g/mol), with a mixture of 5:95 h/d-POO (i.e., their R_g is that of the protonated polymer). With these values, $(\langle R^2 \rangle_0)/M = 0.29 \pm 0.01$ Å² mol/g, which is within the errors equal to the value obtained in the present work.

Fetters and co-workers have examined the relation of the unperturbed chain dimensions of several poly(olefin)s to their molecular weight per backbone bond m_b .¹² They found that this 'backbone equivalence' model (BE model) correctly shows that $\langle R^2 \rangle_0/M$ scales with m_b , but does not produce very exact values.

We have used an analogous expression for the PAO's in ref 20 to get an idea of the chain dimensions and the entanglement molecular weight M_e . With the SANS measurements, it is now possible to calculate the same quantities based on experimental data, and thereby test the quality of the BE model for the PAO's.

In analogy to ref 12, the chain dimensions $\langle R^2 \rangle_0/M$ are calculated as a function of the dimensions of poly(ethylene oxide) (PEO)

$$\frac{\langle R^2 \rangle_0}{M} = \frac{m_{0,PEO}}{m_0} \left(\frac{\langle R^2 \rangle_0}{M} \right)_{PEO} \quad (6)$$

where $m_0 = 3m_b$ is the mass of a monomer.

Table 4. Material Parameters, (a) Deduced from the SANS Data, and (b) Estimated According to Ref 20

	$\langle\langle R^2 \rangle_0\rangle/M$ [\AA^2 mol/g]	p [\AA]	M_e [g/mol]	$d_t = n_t p$ [\AA] ^a	C_∞ ^b
Part a					
PBO	0.48 ± 0.01	3.58 ± 0.07	10600 ± 1200	71.6 ± 3.8	5.38 ± 0.07
PHO	0.34 ± 0.01	5.34 ± 0.01	33900 ± 3400	106.8 ± 5.3	5.22 ± 0.08
POO	0.30 ± 0.01	6.05 ± 0.02	48200 ± 4850	121.0 ± 6.1	5.99 ± 0.36
Part b					
PBO	0.49	3.53	10200	70.6	5.48
PHO	0.35	5.16	30400	103.2	5.48
POO	0.28	6.59	62000	131.8	5.48

^a Tube diameter. ^b Cf. eq 8; for the error calculation it was assumed that N_{mono} is known with an accuracy of ±5.

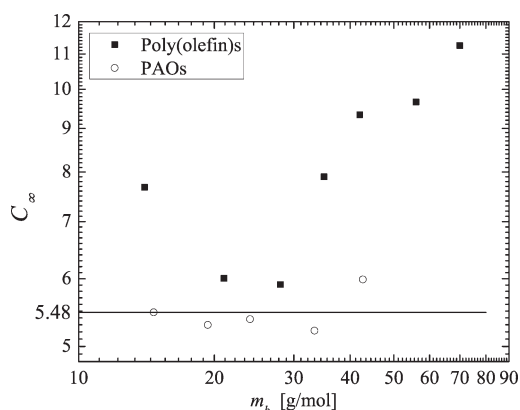


Figure 4. C_∞ vs the mass per backbone bond m_b for poly(olefin)s (filled squares; data taken from ref 10) and PAO's (empty circles). The value for PPO is calculated from ref 2. The line shows the value obtained from the BE model.

The entanglement molecular weight M_e can then be calculated by using

$$M_e = \frac{(n_t p)^2 M}{\langle R^2 \rangle_0} \quad \text{with} \quad p = \frac{M}{\langle R^2 \rangle_0 \rho N_A} \quad (7)$$

p is the so-called packing length⁹ (Witten et al.²⁷ seem to be the first ones to have used this term for their parameter a , which differs from p only by a factor of 3), and n_t is the Ronca-Lin parameter, equal to the number of entanglement strands in a cube with a side length equal to the tube diameter.^{28,29} Taking into account the values we find in the literature,^{9–13} it seems justified to take $n_t = 20 \pm 1$. For PEO, $m_0 = 44$, and $(\langle R^2 \rangle_0/M)_{\text{PEO}} = 0.805 \text{ \AA}^2 \text{ mol/g}$.¹³ The latter value was to our knowledge obtained using R_g 's from Zimm plots.

The derived values resulting from the SANS data (using R_g from the Zimm plots) are listed in Table 4(a). For the calculation of $(\langle R^2 \rangle_0)/M$, $M = M_{w,\text{equiv}}$ has to be used, since the Zimm plot yielded the R_g of the deuterated polymer, but the chain dimensions are actually calculated from the number of monomers.

The results of eq 6 and eq 7 are given in Table 4(b). The values for p , d_t , and M_e are recalculated as compared to ref 20, since there $n_t = 19$ and the mass density ρ at 273 K has been used.

One can see that the values for $(\langle R^2 \rangle_0)/M$ from measurement and calculation agree very well within the error-bars. For the deduced values p , M_e , and d_t experiment and calculation agree in most cases, or are close to each other. The largest deviations

Table 5. Molecular Weight per Backbone Bond m_b of PAO's and Poly(olefin)s

no. of C ^a	PAO's	m_b [g/mol]	poly(olefin)s	m_b [g/mol]
0	PEO	14.67	poly(ethylene)	14.00
1	PPO	19.33	poly(propylene)	21.00
2	PBO	24.00	poly(ethylene)	28.00
3			poly(pentene)	35.00
4	PHO	33.33	poly(hexene)	42.00
6	POO	42.67	poly(octene)	56.00
8			poly(decene)	70.00
10	PDO	61.33		

^a Number of carbon atoms per side chain.

occur for POO, i. e. for the PAO with the longest side chain. We would like to emphasize that in all cases the correct tendency was predicted, and the absolute values are astonishingly close!

The small deviations become more visible when looking at the characteristic ratio C_∞ , which can be regarded as a measure of the stiffness of a polymer chain. C_∞ can be written as (cf. eq 3)

$$C_\infty = \frac{6R_g^2}{N_{\text{mono}} n_b \langle l_0^2 \rangle} = \frac{\langle R^2 \rangle_0 m_b}{M \langle l_0^2 \rangle} \quad (8)$$

For the poly(alkylene oxide)s, $n_b \langle l_0^2 \rangle = 6.46 \text{ \AA}^2$, and we obtain the values given in the last column of Table 4. Inserting eq 6 results in a constant $C_\infty = C_\infty(\text{PEO})$ for all PAO's.

It is interesting that $(\langle R^2 \rangle_0)/M$ of the PAO's decreases as m_b increases in such a way that the resulting $C_\infty \propto (\langle R^2 \rangle_0)/M m_b$ is only slightly increasing, whereas a completely different picture shows up for the poly(olefin)s, as visualized in Figure 4. While C_∞ of the PAO's is around the constant line obtained from the BE model, the poly(olefin)s show a fishhook-like behavior of C_∞ . This means that poly(propylene) and poly(ethylene) appear more flexible than poly(ethylene) but the higher homologues become increasingly stiff, while the PAO's do have a similar flexibility for all side-chain lengths. For better orientation, a list of m_b of the PAO's and poly(olefin)s is given in Table 5.

The fact that C_∞ changes less strongly for the PAO's can be understood qualitatively by taking into account that their C–C–O backbone repeat unit is in itself more flexible than the C–C backbone of the poly(olefin)s. In a more hand-waving fashion, one could say that due to the oxygen atom there is more

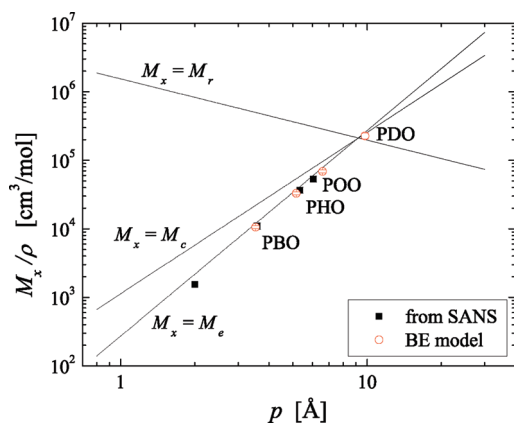


Figure 5. M_x/ρ vs packing length p for $x = e, c,$ and r . The lines are fits to the data of many polymers and are based on data from ref 10; the open circles are the estimated values for the PAO's, the closed squares correspond to the values originating from the SANS data (PEO data taken from ref 11).

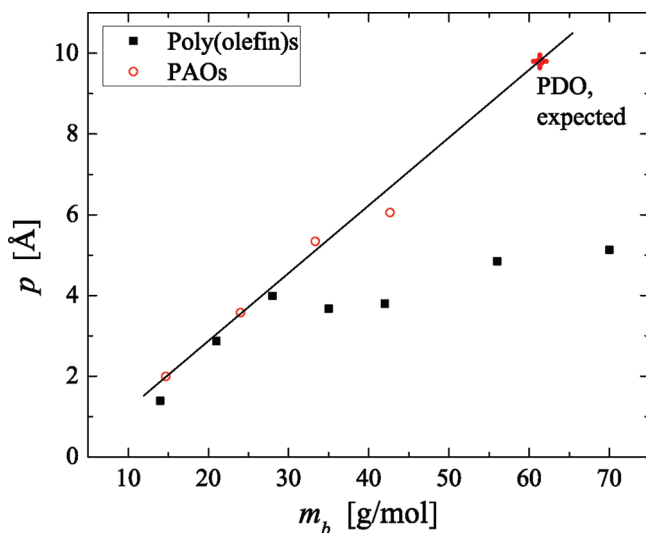


Figure 6. Packing length p vs molecular weight per backbone bond m_b for poly(olefin)s and PAO's; the values for the poly(olefin)s and for poly(ethylene oxide) are taken from ref 12. The line shows the expectation from the BE model.

space for the side chains alongside the backbone in the case of the PAO's, and therefore the coiling of the chain is less inhibited than in the case of the poly(olefin)s.

Since the estimate was rather accurate, one can dare to give values for a PAO with even longer side chain: poly(dodecene oxide) (PDO) has 10 carbon atoms in each n -alkyl side chain, thus $m_b = 61.33$. The density of PDO at 310 K is $\rho = 0.88$ g/cm³, and with this the BE model gives $\langle R^2 \rangle_0/M \approx 0.19$ Å² mol/g. The expected entanglement molecular weight is $M_e \approx 200 \pm 20$ kg/mol, and the packing length should be $p \approx 9.8$ Å. The latter makes PDO a highly interesting polymer, since it is expected that M_e , the critical molecular weight M_c (i.e., where $\eta_0 \propto M$ changes to $\eta_0 \propto M^{3.4}$), and the reptation molecular weight M_r (i.e., where $\eta_0 \propto M^{3.4}$ changes to $\eta_0 \propto M^3$) coincide for polymers with $p = p^* \approx 9.2$ Å.¹⁰ This is visualized in Figure 5. In the picture of the tube model, this means that the contour-length fluctuation

regime is missing and the limit of pure reptation is reached as soon as entanglements are present.

The packing length increases as a function of m_b , as is shown in Figure 6. For the very short side chains, the slope is almost identical for the poly(olefin)s and the PAO's, but then the poly(olefin)-values seem to saturate. The PAO-slope remains virtually unchanged (at least up to the estimated value for PDO) and follows the line that would be expected from the BE model using the appropriate densities. It has to be concluded that the BE model is by no means a perfect description of the static properties of side-chain polymers, but that, other than the poly(olefin)s, the PAO's can be reasonably well approximated.

A possible explanation for the obviously different behavior of the poly(olefin)s and PAO's may be given by the so-called generalized anomeric effect:^{30,31} It is commonly found that there is a much higher probability for gauche conformations when in a sequence of C atoms an atom with lone pair electrons is present. This is the case for the PAO's, and it is therefore understandable that the radius of gyration depends only very little on temperature compared to polymers with pure carbon backbones: for instance it is found that R_g of poly(ethylene propylene) decreases by $\sim 4\%$ when increasing the temperature by 100 K, the temperature coefficient being $\kappa = -1.16 \times 10^{-3}$ K⁻¹.⁶ This effect is attributed to the increased population of the gauche conformation with increased temperature. When the gauche conformation is now favored even at low temperatures, there may be either no change in R_g or it might also increase, depending on the shape of the rotation potential. For PEO, κ is found to be -3.0×10^{-4} K⁻¹,³² which is by far smaller than the PEP value. Hamley et al.²¹ found R_g of POO independent of temperature between room temperature and 178 °C. These findings indicate that the rotational potentials of the PAO's are such that changes in temperature have almost no effect on the chain dimensions. Furthermore, the accessibility of many conformational states should make the chains more flexible and can therefore account for the rather small characteristic ratio.

SUMMARY

We reported the synthesis of deuterated alkylene oxide monomers, and small-angle neutron scattering measurements on three different poly(alkylene oxide)s. The latter showed a systematic decrease of $\langle R^2 \rangle_0/M$ with increasing length of the side chains, and concurred in an almost-quantitative fashion with the values obtained from the very simple backbone equivalence model.^{12,20} On the basis of the good agreement, a prediction of the chain properties of poly(dodecene oxide) is featured, giving reason for the assumption that this polymer has a packing length very close to the value where $M_e = M_c = M_r$ is expected. The qualitatively different behavior of the characteristic ratio of the poly(alkylene oxide)s and the poly(olefin)s is discussed in terms of the molecular mass per backbone bond and the generalized anomeric effect, which may give at least a qualitative reason for the observations.

ASSOCIATED CONTENT

S Supporting Information. Table with all detected components after the hexenoxide synthesis and mass spectrum of hexenoxide-D12 with peak interpretation. This material is available free of charge via the Internet at <http://pubs.acs.org>.

AUTHOR INFORMATION

Corresponding Author

*E-mail: g.j.schneider@fz-juelich.de.

ACKNOWLEDGMENT

We thank Lewis Fetters for his valuable comments. C.G. acknowledges financial support by the International Helmholtz Research School of Biophysics and Soft Matter (IHRS BioSoft).

REFERENCES

- (1) Fox, T. G. *Polymer* **1962**, *3*, 111.
- (2) Matsushima, M.; Fukatsu, M.; Kurata, M. *B. Chem. Soc. Jpn.* **1968**, *41*, 2570.
- (3) Booth, C.; Orme, R. *Polymer* **1970**, *11*, 626.
- (4) Kirste, R. G.; Kruse, W. A.; Ibel, K. *Polymer* **1975**, *16*, 120.
- (5) Xu, Z.; Hadjichristidis, N.; Fetters, L. J. *Macromolecules* **1984**, *17*, 2303.
- (6) Zirkel, A.; Richter, D.; Pyckhout-Hintzen, W.; Fetters, L. J. *Macromolecules* **1992**, *25*, 954.
- (7) Lee, J. S.; Kim, S. C.; Lee, H. K. *Macromol. Res.* **2008**, *16*, 631.
- (8) Dinċ, C. Ö.; Kibarar, G.; Güner, A. *J. Appl. Polym. Sci.* **2010**, *117*, 1100.
- (9) Fetters, L. J.; Lohse, D. J.; Richter, D.; Witten, T. A.; Zirkel, A. *Macromolecules* **1994**, *27*, 4639.
- (10) Fetters, L. J.; Lohse, D. J.; Milner, S. T.; Graessley, W. W. *Macromolecules* **1999**, *32*, 6847.
- (11) Fetters, L. J.; Lohse, D. J.; Graessley, W. W. *J. Polym. Sci., Part B: Polymer Physics* **1999**, *37*, 1023.
- (12) Fetters, L. J.; Lohse, D. J.; García-Franco, C. A.; Brant, P.; Richter, D. *Macromolecules* **2002**, *35*, 10096.
- (13) Fetters, L. J.; Lohse, D. J.; Colby, R. H. In *Physical Properties of Polymers Handbook*, 2nd ed.; Mark, J. E., Ed.; Springer: New York, 2007.
- (14) Graessley, W. W. *Polymeric Liquids & Networks: Structure and Properties*; GS Garland Science, Taylor & Francis Group: New York, London, 2004.
- (15) Andrews, R. J.; Grulke, E. A. In *Polymer Handbook*, 4th ed.; Brandrup, J., Immergut, E. H., Grulke, E. A., Eds.; John Wiley & Sons, Inc.: Hoboken, NJ, 1999.
- (16) Garwe, F.; Schönhals, A.; Lockwenz, H.; Beiner, M.; Schröter, K.; Donth, E. *Macromolecules* **1996**, *29*, 247.
- (17) Beiner, M. *Macromol. Rapid Commun.* **2001**, *22*, 869.
- (18) Hiller, S.; Pascui, O.; Budde, H.; Kabisch, O.; Reichert, D.; Beiner, M. *New J. Phys.* **2004**, *10*, 10.
- (19) Arbe, A.; Genix, A.-C.; Colmenero, J.; Richter, D.; Fouquet, P. *Soft Matter* **2008**, *4*, 1792.
- (20) Gerstl, C.; Schneider, G. J.; Pyckhout-Hintzen, W.; Allgaier, J.; Richter, D.; Alegria, A.; Colmenero, J. *Macromolecules* **2010**, *43*, 4968–4977.
- (21) Hamley, I. W.; O'Driscoll, B. M. D.; Lotze, G.; Moulton, C.; Allgaier, J.; Frielinghaus, H. *Macromol. Rapid Commun.* **2009**, *30*, 2141.
- (22) Allgaier, J.; Willbold, S.; Chang, T. *Macromolecules* **2007**, *40*, 518.
- (23) http://www.jcns.info/jcns_kws1/.
- (24) Higgins, J. S.; Benoit, H. C. *Polymers and Neutron Scattering*; Clarendon Press: Oxford, 1994.
- (25) Haynes, W. M.; Lide, D. R.; et al., *CRC Handbook of Chemistry and Physics*, 91st ed.; Taylor and Francis Group, LLC: 2011; (Internet Version 2011).
- (26) Nusser, K.; Neueder, S.; Schneider, G. J.; Meyer, M.; Pyckhout-Hintzen, W.; Willner, L.; Radulescu, A.; Richter, D. *Macromolecules* **2010**, *43*, 9837.
- (27) Witten, T. A.; Milber, S. T.; Wang, Z.-G. In *Multiphase Macromolecular Systems*; Culbertson, B. M., Ed.; Plenum: New York, 1989.
- (28) Ronca, G. *J. Chem. Phys.* **1983**, *79*, 1031.
- (29) Lin, Y.-H. *Macromolecules* **1987**, *20*, 3080.
- (30) Thatcher, G. R. J., Ed. *The Anomeric Effect and Associated Stereoelectronic Effects*; American Chemical Society: Washington, DC, 1993; pp 6–25.
- (31) Tvaroska, I.; Beha, T. *Can. J. Chem.* **1979**, *57*, 424.
- (32) Smith, G. D.; Yoon, D. Y.; Jaffe, R. L.; Colby, R. H.; Krishnamoorti, R.; Fetters, L. J. *Macromolecules* **1996**, *29*, 3462.